

## Comments by editor

Thank you for addressing the comments. I did a quick review of the revised manuscript. It appears that Table 1, which is summarized and referred to in lines 82-88, is incomplete. A couple of GCM studies mentioned in the text are missing from the table. Also, Koch and Hansen (2005) is a GCM study rather than a CTM study (line 86). Please make the corrections and upload a revised manuscript for publication.

Response: We appreciate for your effect in another review. GCM studies mentioned in the text are now added in Table 1 for comparison, and corresponding references updated. Koch and Hansen (2005) is placed in line with GCM in lines 85-87 as "...chemical transport models (Ikeda et al., 2017; Qi et al., 2017; Shindell et al., 2008; Wang et al., 2011; Xu et al., 2017), and global climate models (Ma et al., 2013; Koch and Hansen, 2005; Schacht et al., 2019; H. Wang et al., 2014) (Table 1)".

Table 1. Comparison of BC source contributions in the Arctic surface

Model and versions	Model type	Wet-deposition	Grid resolution	Meteorology	Emissions	Domain/Sites	Year/season	Major source regions/sectors	Reference
Flexpart-WRF 6.2	Lagrangian	Stohl et al. (2005)	unspecified	WRF forecast	ECLIPSE, FINN	continental Norway and Svalbard	spring 2013	Asian anthropogenic	Liu et al. (2015)
Flexpart 6.2	Lagrangian	Stohl et al. (2005)	1° × 1°	ECMWF operational	Unspecified (BC sensitivities were calculated)	Alert, Barrow, Zeppelin	1989-2009	Northern Eurasia	Hirdman et al. (2010)
Flexpart 6.2	Lagrangian	Stohl et al. (2005)	1° × 1°	ECMWF operational	ECLIPSE4(GAINS), GFED3	Arctic (north of 66°N)	2008-2010	Flaring (42%), residential (>20%)	Stohl et al. (2013)
Flexpart 9.2	Lagrangian	Stohl et al. (2005)	1° × 1°	ECMWF operational	ECLIPSE5(GAINS), GFED4.1	Arctic (north of 66.7°N)	2011-2015	Residential and open burning (39%)	Winiger et al. (2019)
Flexpart 10.1	Lagrangian	Grythe et al. (2017)	1° × 1°	ECMWF operational	HTAP2, GFED3, Huang et al. (2015) for Russia flaring	Arctic (north of 66°N)	2010	Flaring (36%), open burning (18%), residential (15%), others (31%)	Current study
GEOS-Chem 9.02	CTM	Wang et al. (2011)	2° × 2.5°	GEOS-5	HTAP2, GFED3, Huang et al. (2015) for Russia flaring	Arctic (north of 66°N)	2007-2011	Russia (62%)	Ikeda et al. (2017)
GEOS-Chem	CTM	Wang et al. (2011)	2° × 2.5°	GEOS-5	Bond et al. (2004), Zhang et al. (2009), GFED3	Alert, Barrow, Zeppelin	April 2008	Asian anthropogenic (35–45%), Siberian biomass burning (46–64%)	Qi et al. (2017)
GEOS-Chem	CTM	Wang et al. (2011)	2° × 2.5°	GEOS-5	Bond et al. (2007), FLAMBE	North America Arctic	April 2008	Open fire (50%)	Wang et al. (2011)
GEOS-Chem10.01	CTM	Wang et al. (2011)	2° × 2.5°	GEOS-5	HTAP2, ECLIPSE5, GFED4	Alert, Barrow, Zeppelin, Arctic (north of 66.5°N)	2009-2011	Northern Asian anthropogenic (40–45%) in winter-spring	Xu et al. (2017)
CAMS5	GCM	Wang et al. (2013)	1.9° × 2.5°	MERRA	IPCC AR5	Arctic (north of 66.5°N)	1996-2005	Northern Europe in winter, Northern Asia in summer	Wang et al. (2014)
CAMS5	GCM	Wang et al. (2013)	1.9° × 2.5°	Free running CAM5, ERA-Interim	POLARCAT-POLMIP	Arctic (north of ~66°N)	Winter 2008	Asia	Ma et al. (2013)
ECHAM-HAM	GCM	Zhang et al. (2012)	1.8° × 1.8°	ERA-Interim	ECLIPSE5, and Huang et al. (2015) for anthropogenic BC in Russia (default), GFES, and comparison with ACCMIP	Various sites and aircraft campaigns, Arctic (north of 60°N)	2005–2015	Northern Asia, Northern Europe, Russian gas flaring region (with default emission)	Schacht et al. (2019)
GISS ModelE	GCM	Koch et al. (2006)	4° × 5°	Internal	Bond et al. (2004), Cooke and Wilson (1996)	Arctic (north of ~60°N)	Annual general	South Asia	Koch and Hansen (2005)

1 **Flexpart v10.1 simulation of source contributions to Arctic black carbon**

2

3 Chunmao Zhu<sup>1</sup>, Yugo Kanaya<sup>1,2</sup>, Masayuki Takigawa<sup>1,2</sup>, Kohei Ikeda<sup>3</sup>, Hiroshi Tanimoto<sup>3</sup>,

4 Fumikazu Taketani<sup>1,2</sup>, Takuma Miyakawa<sup>1,2</sup>, Hideki Kobayashi<sup>1,2</sup>, Ignacio Pissó<sup>4</sup>

5

6 <sup>1</sup>Research Institute for Global Change, Japan Agency for Marine–Earth Science and  
7 Technology (JAMSTEC), Yokohama 2360001, Japan

8 <sup>2</sup>Institute of Arctic Climate and Environmental Research, Japan Agency for Marine–Earth  
9 Science and Technology, Yokohama 2360001, Japan

10 <sup>3</sup>National Institute for Environmental Studies, Tsukuba 305-8506, Japan

11 <sup>4</sup>NILU – Norwegian Institute for Air Research, Kjeller 2027, Norway

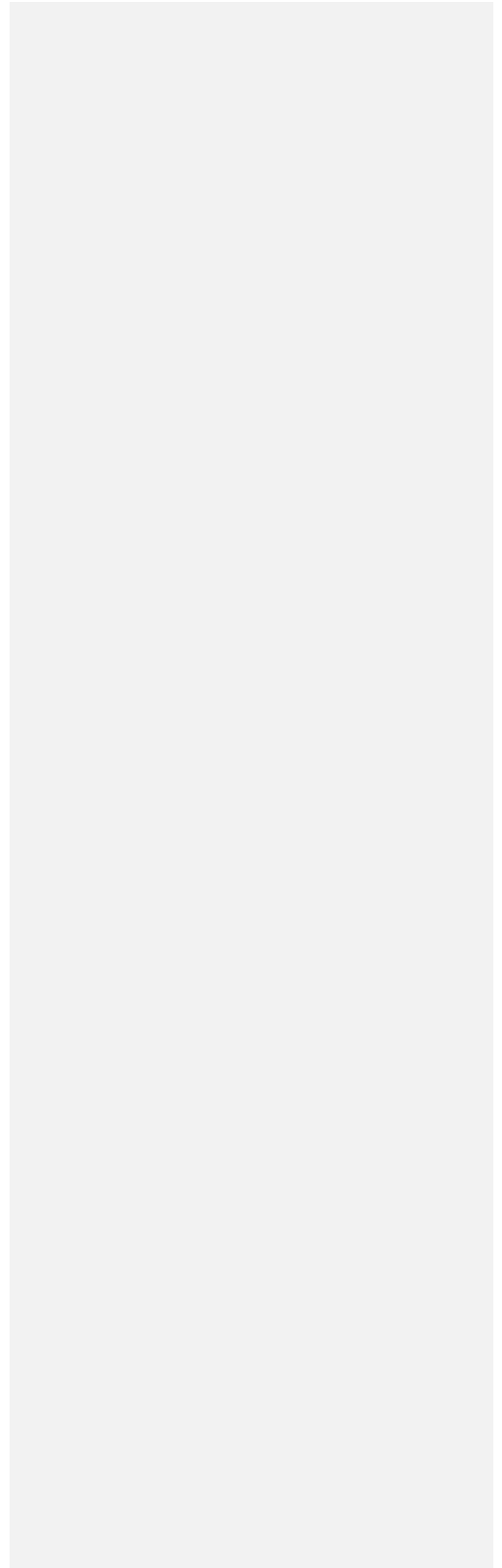
12

13 Correspondence to Chunmao Zhu (chmzhu@jamstec.go.jp)

## 14      **Abstract**

15      The Arctic environment is undergoing rapid changes such as faster warming than the  
16 global average and exceptional melting of glaciers in Greenland. Black carbon (BC) particles,  
17 which are a short-lived climate pollutant, are one cause of Arctic warming and glacier  
18 melting. However, the sources of BC particles are still uncertain. We simulated the potential  
19 emission sensitivity of atmospheric BC present over the Arctic (north of 66° N) using the  
20 Flexpart Lagrangian transport model (version 10.1). This version includes a new aerosol wet  
21 removal scheme, which better represents particle-scavenging processes than older versions  
22 did. Arctic BC at the surface (0–500 m) and high altitudes (4750–5250 m) is sensitive to  
23 emissions in high latitude (north of 60° N) and mid-latitude (30–60° N) regions, respectively.  
24 Geospatial sources of Arctic BC were quantified, with a focus on emissions from  
25 anthropogenic activities (including domestic biofuel burning) and open biomass burning  
26 (including agricultural burning in the open field) in 2010. We found that anthropogenic  
27 sources contributed 82 % and 83 % of annual Arctic BC at the surface and high altitudes,  
28 respectively. Arctic surface BC comes predominantly from anthropogenic emissions in  
29 Russia (56 %), with gas flaring from the Yamalo-Nenets Autonomous Okrug and Komi  
30 Republic being the main source (31 % of Arctic surface BC). These results highlight the need  
31 for regulations to control BC emissions from gas flaring to mitigate the rapid changes in the  
32 Arctic environment. In summer, combined open biomass burning in Siberia, Alaska, and  
33 Canada contributes 56–85 % (75 % on average) and 40–72 % (57 %) of Arctic BC at the  
34 surface and high altitudes, respectively. A large fraction (40 %) of BC in the Arctic at high  
35 altitudes comes from anthropogenic emissions in East Asia, which suggests that the rapidly  
36 growing economies of developing countries could have a non-negligible effect on the Arctic.  
37 To our knowledge, this is the first year-round evaluation of Arctic BC sources that has been

38 performed using the new wet deposition scheme in Flexpart. The study provides a scientific  
39 basis for actions to mitigate the rapidly changing Arctic environment.  
40



## 41 1 Introduction

42 The Arctic region has experienced warming at a rate twice that of the global average in  
43 recent decades (Cohen et al., 2014). The Arctic cryosphere has been undergoing  
44 unprecedented changes since the mid-1800s (Trusel et al., 2018). Glacier cover in Greenland  
45 reached its historically lowest level in summer 2012 (Tilling et al., 2015). Evidence indicates  
46 that the emissions and transport of greenhouse gases and aerosols to the Arctic region are  
47 contributing to such warming and melting of snow and ice (Keegan et al., 2014; Najafi et al.,  
48 2015). Short-lived climate pollutants such as black carbon (BC) particles (e.g., Sand et al.,  
49 2016; Yang et al., 2019), sulfate aerosol (Yang et al., 2018), tropospheric ozone, and  
50 methane greatly affect the Arctic climate (AMAP, 2015; Quinn et al., 2008).

51 BC particles are emitted during incomplete combustion of fossil fuels, biofuels, and  
52 biomass. BC warms the atmosphere by direct absorption of solar radiation. The deposition  
53 of BC on snow and ice surfaces accelerates their melting through decreasing albedo, which  
54 contributes to the rapid loss of glaciers. In the Arctic region, ground-based observations  
55 have indicated that BC shows clear seasonal variations, with elevated mass concentrations  
56 in winter and spring (the so-called Arctic haze) and low values in summer (Law and Stohl,  
57 2007). Such seasonal variations are explained by increased transport from lower latitudes in  
58 the cold season and increased wet scavenging in the warm season (Shaw, 1995; Garrett et  
59 al., 2011; Shen et al., 2017).

60 The presence of BC particles in the Arctic is mainly attributed to emissions in high-latitude  
61 regions outside the Arctic, such as northern Europe and Russia (Stohl, 2006; Brock et al.,  
62 2011). This is partly caused by the polar dome (Stohl, 2006), which is formed because of the  
63 presence of constant potential temperature near the surface. The emissions in high-latitude  
64 regions are transported to the Arctic region and trapped in the dome, which increases the

65 surface concentration. Recently, Schmale et al. (2018) suggested that local emissions from  
66 within the Arctic are another important source, and these are expected to increase in the  
67 future.

68 Although numerous studies have been performed, results regarding regional  
69 contributions of BC sources in the Arctic are still inconclusive. For example, ground-based  
70 observations and Lagrangian transport model results reported by Winiger et al. (2016)  
71 showed that BC in Arctic Scandinavia is predominantly linked to emissions in Europe. Over  
72 the whole Arctic region (north of 66° N), Russia contributes 62 % to surface BC in terms of  
73 the annual mean (Ikeda et al., 2017). Gas flaring in Russia has been identified as a major  
74 (42 %) source of BC at the Arctic surface (Stohl et al., 2013). Xu et al. (2017) found that  
75 anthropogenic emissions from northern Asia contribute 40–45 % of Arctic surface BC in  
76 winter and spring. However, the results of some other studies have suggested that Russia,  
77 Europe, and South Asia each contribute 20–25 % of BC to the low-altitude springtime Arctic  
78 haze (Koch and Hansen, 2005). Sand et al. (2016) found that the surface temperature in the  
79 Arctic is most sensitive to emissions in Arctic countries, and Asian countries contribute  
80 greatly to Arctic warming because of the large absolute amount of emissions. With these  
81 large disagreements among studies, it is thus necessary to unveil BC sources in the Arctic  
82 with high precision simulations.

83 Various models have been used to investigate BC sources in the Arctic. Depending on the  
84 simulation method, these models are generally categorized as Lagrangian transport models  
85 (Hirdman et al., 2010; Liu et al., 2015; Stohl et al., 2006, 2013), chemical transport models  
86 (Ikeda et al., 2017; Qi et al., 2017; Shindell et al., 2008; Wang et al., 2011; Xu et al., 2017),  
87 and global climate models (Ma et al., 2013; [Koch and Hansen, 2005](#); Schacht et al., 2019; H.  
88 Wang et al., 2014) (Table 1). The treatment of wet-scavenging parameterizations is a key

Deleted: Koch and Hansen, 2005;

90 factor affecting the model performance, which determines the uncertainties related to BC  
91 particle removal (Kipling et al., 2013; Schacht et al., 2019; Q. Wang et al., 2014). The use of  
92 emission inventories is another important factor that affects the simulation results (Dong et  
93 al., 2019). The observations of BC that are used for model comparisons may be biased by a  
94 factor of 2 depending on the method used (Sinha et al., 2017; Sharma et al., 2017). There  
95 are still large uncertainties regarding the sources of BC in the Arctic with respect to emission  
96 sectors (anthropogenic sources and open biomass burning) and geospatial contributions  
97 (Eckhardt et al., 2015).

98 The FLEXible PARTicle dispersion model (Flexpart) had been used to investigate the  
99 transport pathways and source contributions of BC in the Arctic (Stohl et al., 1998, 2006,  
100 2013). Of Flexpart model up to version 9, wet removal was treated considering below-cloud  
101 and within-cloud scavenging processes (Hertel et al., 1995; McMahon and Denison, 1979),  
102 which depends on cloud liquid water content, precipitation rate and the depth of the cloud.  
103 However, clouds were parameterized based on relative humidity, clouds frequently  
104 extended to the surface and at times no clouds could be found in grid cells, with unrealistic  
105 precipitation (Grythe et al., 2017). Recently, version 10 of Flexpart had been developed in  
106 which cloud is differentiated into liquid, solid, and mixed phase, the cloud distribution is  
107 more consistent with the precipitation data (Grythe et al., 2017). This improvement in the  
108 cloud distribution and phase leads to a more realistic distribution of below-cloud and in-  
109 cloud scavenging events. In this study, we quantified region-separated sources of BC in the  
110 Arctic in 2010 by using Flexpart v10.1. We first evaluated the model performance by  
111 comparing the results with those based on observations at surface sites. The source  
112 contributions of emission sectors and geospatial contributions were evaluated by  
113 incorporating the Arctic BC footprint into the emission inventories.

## 114 **2 Materials and methods**

### 115 2.1 Transport model

116 The Flexpart model (version 10.1) was run in backward mode to simulate BC footprints in  
117 the Arctic region. The calculation of wet deposition was improved compared with those in  
118 previous versions because in-cloud scavenging and below-cloud scavenging of particles were  
119 separately calculated (Grythe et al., 2017). In previous versions of Flexpart, in the in-cloud  
120 scavenging scheme, the aerosol scavenging coefficient depended on the cloud water  
121 content, which was calculated according to an empirical relationship with precipitation rate,  
122 in which all aerosols had the same nucleation efficiency (Hertel et al., 1995 ; Stohl et al.,  
123 2005). In the new version, the in-cloud scavenging scheme depends on the cloud water  
124 phase (liquid, ice, or mixed phase). Aerosols were set as ice nuclei for ice clouds and as  
125 cloud condensation nuclei for liquid-water clouds, respectively. For mixed-phase clouds, it  
126 was assumed that 10 % of aerosols are ice nuclei and 90 % are cloud condensation nuclei,  
127 because BC is much more efficiently removed in liquid water clouds than in ice clouds (Cozic  
128 et al., 2007; Grythe et al., 2017). The below-cloud scavenging scheme can parameterize  
129 below-cloud removal as a function of aerosol particle size, and precipitation type (snow or  
130 rain) and intensity. The biases produced in simulations using the new scheme are therefore  
131 smaller than those in the old scheme for wet deposition of aerosols, especially at high  
132 latitudes (Grythe et al., 2017).

133 The Arctic region is defined as areas north of 66° N. The potential BC emission  
134 sensitivities at two heights in the Arctic region, i.e., the surface (0–500 m) and high altitudes  
135 (4750–5250 m), were simulated. The Flexpart outputs were set as gridded retention times.  
136 We performed tests at 500, 2000, and 5000 m, and chose 500 m as the upper boundary  
137 height of the model output. The model was driven with operational analytical data from the



138 European Centre for Medium-Range Weather Forecasts (ECMWF) at a spatial resolution of  
139  $1^\circ \times 1^\circ$  with 61 vertical levels. Temporally, ECMWF has a resolution of 3 h, with 6 h analysis  
140 and 3 h forecast time steps. The simulation period was set at 60 days backward starting  
141 from each month in 2010. The maximum lifetime of BC was set at 20 days because its  
142 suspension time in the upper atmosphere during long-range transport is longer than that at  
143 the surface level (Stohl et al., 2013). We implemented the wet deposition scheme in the  
144 backward calculations, but it was not represented in the default setting (Flexpart v10.1,  
145 <https://www.flexpart.eu/downloads>, obtained 10 April 2017).

146 The chemistry and microphysics could not be resolved by Flexpart. The model therefore  
147 ignores hydrophobic to hydrophilic state changes and size changes of BC, and assumes that  
148 all BC particles are aged hydrophilic particles. This may lead to an overestimation of BC  
149 removal and hence force underestimation of simulated BC concentration, especially of fossil  
150 fuel combustion sources where BC could be in the hydrophobic state for a few days. A  
151 logarithmic size distribution of BC with a mean diameter of  $0.16 \mu\text{m}$  and a standard  
152 deviation of 1.96, in accordance with our ship observations in the Arctic, was used (Taketani  
153 et al., 2016). The particle density was assumed to be  $2000 \text{ kg m}^{-3}$ , and 1 million  
154 computational particles were randomly generated in the Arctic region for the backward  
155 runs.

156 Four ground-based observations made during the period 2007–2011 were used to  
157 validate the model performance. The potential BC emission sensitivity at 0–500 m above  
158 ground level from a  $0.1^\circ$  grid centered at each site was simulated. Other model  
159 parameterizations were consistent with those for the Arctic region, except that 200 000  
160 computational particles were released.

161 2.2 Emission inventories

162 We focused on BC sources from anthropogenic emissions and open biomass burning. The  
163 Hemispheric Transport of Air Pollution version 2 inventory (HTAP2) for 2010 was used for  
164 monthly anthropogenic BC emissions (Janssens-Maenhout et al., 2015), which include  
165 sectors from energy, industry, residential and transport. It is worth noting that the  
166 residential sector includes not only combustions of fossil fuels, but also biofuels. However,  
167 as it has been reported that BC emissions in Russia were underestimated in HTAP2, we used  
168 the BC emissions reported by Huang et al. (2015) for Russia, in which the annual BC  
169 emissions were 224 Gg yr<sup>-1</sup>. For open biomass burning, we used the monthly BC emissions  
170 from the Global Fire Emissions Database version 3 inventory (GFED3) (van der Werf et al.,  
171 2010) for the purposes of intercomparison with other studies, as this version is widely used.  
172 The term “open biomass burning” here indicates burning of biomass in the open field as is  
173 determined by the remote sensing measurement basis, including forest, agricultural waste,  
174 peat fires, grassland and savanna, woodland, deforestation and degradation, where biofuel  
175 burning for residential use is not included. Geospatial distributions of emissions from  
176 anthropogenic sources and open biomass burning in January and July are shown in Fig. S1.

### 177 2.3 Calculation of Arctic BC source contributions

178 The source contributions to Arctic BC were derived by incorporating the gridded  
179 retention time into the column emission flux, which was derived from the emission  
180 inventories in each grid. Calculations for anthropogenic sources and open biomass burning  
181 were performed separately and the sum was used. For anthropogenic sources, the regions  
182 were separated into North America and Canada (25–80° N, 50–170° W), Europe (30–80° N,  
183 0–30° E), Russia (53–80° N, 30–180° E), East Asia (35–53° N, 75–150° E and 20–35° N, 100–  
184 150° E), and others (the rest) (Fig. 1a). For open biomass burning sources, the regions were

185 separated into Alaska and Canada (50–75° N, 50–170° W), Siberia (50–75° N, 60–180° E),  
186 and others (Fig. 1b).

### 187 2.3 Observations

188 BC levels simulated by Flexpart were compared with those based on surface observations  
189 at four sites: Barrow, USA (156.6° W, 71.3° N, 11 m asl), Alert, Canada (62.3° W, 82.5° N,  
190 210 m asl), Zeppelin, Norway (11.9° E, 78.9° N, 478 m asl), and Tiksi, Russia (128.9° E, 71.6°  
191 N, 8 m asl). Aerosol light absorption was determined by using particle soot absorption  
192 photometers (PSAPs) at Barrow, Alert, and Zeppelin, and an aethalometer at Tiksi. For PSAP  
193 measurements, the equivalent BC values were derived using a mass absorption efficiency of  
194  $10 \text{ m}^2 \text{ g}^{-1}$ . The equivalent BC at Tiksi, which was determined with an aethalometer, was  
195 obtained directly. These measurement data were obtained from the European Monitoring  
196 and Evaluation Programme and World Data Centre for Aerosols database  
197 (<http://ebas.nilu.no>) (Tørseth et al., 2012).

198 It is worth noting that uncertainties could be introduced by using different BC  
199 measurement techniques. An evaluation of three methods for measuring BC at Alert,  
200 Canada indicated that an average of the refractory BC determined with a single-particle soot  
201 photometer (SP2) and elemental carbon (EC) determined from filter samples give the best  
202 estimate of BC mass (Sharma et al., 2017). Xu et al. (2017) reported that the equivalent BC  
203 determined with a PSAP was close to the average of the values for refractory BC and EC at  
204 Alert. In this study, we consider that the equivalent BC values determined with a PSAP at  
205 Barrow, Alert, and Zeppelin to be the best estimate. There may be uncertainties in the  
206 equivalent BC observations performed with an aethalometer at Tiksi because of co-existing  
207 particles such as light-absorptive organic aerosols, scattering particles, and dusts  
208 (Kirchstetter et al., 2004; Lack and Langridge, 2013). Interference by the filter and

209 uncertainties in the mass absorption cross section could also contribute to the bias  
210 observed in measurements made with an aethalometer at Tiksi.

### 211 **3 Results and discussion**

#### 212 **3.1. Comparisons of simulations with BC observations at Arctic surface sites**

213 Flexpart generally reproduced the seasonal variations in BC at four Arctic sites well  
214 [Pearson correlation coefficient ( $R$ ) = 0.53–0.80, root-mean-square error (RMSE) = 15.1–56.8  
215  $\text{ng m}^{-3}$ ] (Fig. 2). Winter maxima were observed for the four sites, while a secondary  
216 elevation was observed for Alert and Tiksi. At Barrow, the observed high values of BC were  
217 unintentionally excluded during data screening in the forest fire season in summer (Stohl et  
218 al., 2013); the original observed BC is supposed to be higher as was reflected by the  
219 simulation. This seasonality is probably related to relatively stronger transport to the Arctic  
220 region in winter, accompanied by lower BC aging and inefficient removal, as simulated by  
221 older versions of Flexpart (Eckhardt et al., 2015; Stohl et al., 2013).

222 From January to May at Barrow and Alert, the mean BC simulated by Flexpart v10.1 were  
223  $32.2 \text{ ng m}^{-3}$  and  $31.2 \text{ ng m}^{-3}$ , respectively. Which was 46 % lower than the observations  
224 ( $59.3 \text{ ng m}^{-3}$  and  $58.2 \text{ ng m}^{-3}$ , respectively). This is probably related to the inadequate BC  
225 emission in the inventory, although seasonal variations in residential heating are included in  
226 HTAP2, which would reduce the simulation bias (Xu et al., 2017). Simulations by GEOS-Chem  
227 using the same emission inventories also underestimated BC levels at Barrow and Alert  
228 (Ikeda et al., 2017; Xu et al., 2017). The underestimation by Flexpart could also be partly  
229 contributed by the assumption that all particles are hydrophilic, where the BC scavenging  
230 could be overestimated. The corresponding uncertainties are larger in winter months, when  
231 there are more sources from fossil fuel combustion.

232 At Zeppelin, the Flexpart-simulated BC ( $39.1 \text{ ng m}^{-3}$  for annual mean) was 85 % higher  
233 than the observed value ( $21.1 \text{ ng m}^{-3}$  for annual mean), especially in winter (112% higher). It  
234 has been reported that riming in mixed-phase clouds occurs frequently at Zeppelin (Qi et al.,  
235 2017). During the riming process, BC particles act as ice particles and collide with the  
236 relatively numerous water drops, which form frozen cloud droplets, and then snow is  
237 precipitated. This results in relatively efficient BC scavenging (Hegg et al., 2011). Such a  
238 process could not be dealt with by the model. At Tiksi, Flexpart underestimated BC ( $74.4 \text{ ng}$   
239  $\text{m}^{-3}$  for annual mean) in comparison with observation ( $104.2 \text{ ng m}^{-3}$  for annual mean). Other  
240 than the hydrophilic BC assumption and underestimated BC emission in the simulation as  
241 the cases for Barrow and Alert, the observations at Tiksi by an aethalometer could  
242 contain light-absorbing particles other than BC, resulting in higher observed  
243 concentrations if compared with those obtained by SP2, EC and PSAP.

244 Anthropogenic emissions are the main sources of BC at the four Arctic sites from late  
245 autumn to spring, whereas open biomass burning emissions make large contributions in  
246 summer. From October to April, anthropogenic emissions accounted for 87–100 % of BC  
247 sources at all the observation sites. At Barrow, open biomass burning accounted for 35–  
248 78 % of BC in June–September (Fig. 2). There are large interannual variations in both  
249 observed and simulated BC (Fig. S2). In June–August 2010, the mean contributions of open  
250 biomass burning to BC were 6.3, 2.4, and 8.6 times those from anthropogenic sources at  
251 Alert, Zeppelin, and Tiksi, respectively. In this study, we focused on BC in the Arctic region in  
252 2010.

### 253 **3.2 Potential emission sensitivity of Arctic BC**

254 The potential emission sensitivities (footprint) of Arctic BC showed different patterns  
255 with respect to altitude. The Arctic surface is sensitive to emissions at high latitudes ( $>60^\circ$

256 N). Air masses stayed for over 60 s in each of the 1° grids from the eastern part of northern  
257 Eurasia and the Arctic Ocean before being transported to the Arctic surface in the winter,  
258 represented by January (Fig. 3a). In comparison, during the summer, represented by July, BC  
259 at the Arctic surface was mainly affected by air masses that originated from the Arctic  
260 Ocean and the Norwegian Sea (Fig. 3b). These results imply that local BC emissions within  
261 the Arctic regions, although relatively weak compared with those from the mid-latitude  
262 regions, could strongly affect Arctic air pollution. Local BC emissions are important in the  
263 wintertime because the relatively stable boundary layer does not favor pollution dispersion.  
264 Recent increases in anthropogenic emissions in the Arctic region, which have been caused  
265 by the petroleum industry and development of the Northern Sea Route, are expected to  
266 cause deterioration of air quality in the Arctic. Socio-economic developments in the Arctic  
267 region would increase local BC emissions, and this will be a non-negligible issue in the future  
268 (Roiger et al., 2015; Schmale et al., 2018).

269 BC at high altitudes in the Arctic is more sensitive to mid-latitude (30–60° N) emissions,  
270 especially in wintertime. In January, air masses hovered over the Bering Sea and the North  
271 Atlantic Ocean before arriving at the Arctic (Fig. 3c). A notable corridor at 30–50° N covering  
272 Eurasia and the United States was the sensitive region that affected BC at high altitudes in  
273 the Arctic in January. These results indicate that mid-latitude emissions, especially those  
274 with relatively large strengths from East Asia, East America, and Europe, could alter the  
275 atmospheric constituents at high altitudes in the Arctic. Central to east Siberia was the most  
276 sensitive region for BC at high altitudes in the Arctic in July (Fig. 3d). These results suggest  
277 that pollutants from frequent and extensive wildfires in Siberia in summer are readily  
278 transported to high altitudes in the Arctic. Boreal fires are expected to occur more  
279 frequently and over larger burning areas under future warming (Veira et al., 2016),

280 therefore the atmospheric constituents and climate in the Arctic could undergo more rapid  
281 changes.

### 282 **3.3 Seasonal variations and sources of Arctic surface BC**

283 Arctic surface BC showed clear seasonal variations, with a primary peak in winter–spring  
284 (December–March, 61.8–82.8 ng m<sup>-3</sup>) and a secondary peak in summer (July, 52.7 ng m<sup>-3</sup>).  
285 BC levels were relatively low in May–June (21.8–23.1 ng m<sup>-3</sup>) and September–November  
286 (34.1–40.9 ng m<sup>-3</sup>) (Fig. 4a). This seasonality agrees with observations and simulations at  
287 Alert, Tiksi, and Barrow if consider the unintentional data exclusion (Stohl et al., 2013), and  
288 previous studies targeting the whole Arctic (Ikeda et al., 2017; Xu et al., 2017). Compared  
289 with the study reported by Stohl et al. (2013), the current work using the new scheme  
290 produced smaller discrepancies between the simulated data and observations. Although the  
291 simulation periods (monthly means for 2007–2011 in this study and for 2008–2010 in the  
292 old scheme) and the anthropogenic emission inventories (HTAP2 in this study and ECLIPSE4  
293 in the previous study) are different, the new scheme shows potential for better representing  
294 BC transport and removal processes in the Arctic.

295 The annual mean Arctic BC at the surface was estimated to be 48.2 ng m<sup>-3</sup>. From October  
296 to April, anthropogenic sources accounted for 96–100 % of total BC at the Arctic surface.  
297 Specifically, anthropogenic emissions from Russia accounted for 61–76 % of total BC in  
298 October–May (56 % annually), and was the dominant sources of Arctic BC at the surface.  
299 From an isentropic perspective, the meteorological conditions in winter favored the  
300 transport of pollutants from northern Eurasia to the lower Arctic, along with diabatic cooling  
301 and strong inversions (Klonecki et al., 2003). In comparison, open biomass burning from  
302 boreal regions accounted for 56–85 % (75 % on average) of Arctic BC at the surface in  
303 summer; open biomass burning emissions from North America and Canada accounted for

304 54 % of total Arctic surface BC in June, and those from Siberia accounted for 59–61 % in  
305 July–August. Wildfires in the boreal forests in summer had a major effect on air quality in  
306 the Arctic.

307 On an annual basis, anthropogenic sources and open biomass burning emissions  
308 accounted for 82 % and 18 %, respectively, of total Arctic surface BC. In which, gas flaring  
309 and residential burning (including burning of fossil fuels and biofuels) are accounting for  
310 36 % (28–57 % in October–March) and 15 % (13–25 % in October–March), respectively (Fig.  
311 5a-b). Our results support Stohl et al. (2013) that residential combustion emissions,  
312 especially in winter are important sources of Arctic BC (Table 1). We estimated a  
313 contribution of gas flaring to Arctic surface BC of  $17.5 \text{ ng m}^{-3}$  (36% of total). In comparison,  
314 the value was estimated as  $11.8 \text{ ng m}^{-3}$  using an average Arctic surface BC of  $28 \text{ ng m}^{-3}$  and  
315 a fraction from gas flaring of 42 % evaluated by earlier versions of Flexpart (Stohl et al.,  
316 2013; Winiger et al., 2019). The different contribution could be partly attributed to the  
317 difference in gas flaring emission inventory. BC emission from gas flaring in Russia by Huang  
318 et al. (2015) was used in the current study, where total BC emission from gas flaring in  
319 Russia in 2010 was ca. 81.1 kilotonne, which was larger than the estimate of ca. 64.9  
320 kilotonne by GAINS inventory (Klimont et al., 2017) used by Stohl et al. (2013). Moreover,  
321 Adopting ECLIPSEv5 inventory as was used by Winiger et al. (2019), we estimated that gas  
322 flaring was contributing  $14.4 \text{ ng m}^{-3}$  to Arctic surface BC using Flexpart v10.1, a value 22 %  
323 higher than those obtained using Flexpart v9. This difference could be attributed to the  
324 improvement of the wet-scavenging scheme by Flexpart v10.1.

325 A recent study based on isotope observations at the Arctic sites and Flexpart v9.2  
326 simulation suggested that open biomass burning, including open field burning and  
327 residential biofuel burning, contributed 39 % of annual BC in 2011–2015 (Winiger et al.,



328 2019) (Table 1). In comparison, we estimated that residential burning and open biomass  
329 burning together account for 33 % of total Arctic surface BC. As the residential burning in  
330 our study includes burning of both biofuels and fossil fuels, our results indicated that  
331 biomass burning has a relatively smaller contribution. Other than the differences in BC  
332 removal treatment between different versions of the model, the contribution difference  
333 could also be attributed to the different emission inventories and years (2010 versus 2011-  
334 2015).

335 The geospatial contributions of anthropogenic sources and open biomass burning  
336 emissions can be further illustrated by taking January and July as examples. In January, high  
337 levels of anthropogenic emissions from Russia (contributing 64 % of Arctic surface BC),  
338 Europe (18 %), and East Asia (9 %) were identified (Fig. 6a). Specifically, Yamalo-Nenets  
339 Autonomous Okrug in Russia, which has the largest reserves of Russia's natural gas and oil  
340 (Filimonova et al., 2018), was the most notable emission hotspot, which suggests gas-flaring  
341 sources. The Komi Republic in Russia was also identified as a strong anthropogenic emitter  
342 contributing to Arctic surface BC. These gas-flaring industrial regions in Russia (58–69° N,  
343 68–81°E) together contributed 33 % and 31 % of Arctic surface BC for January and the  
344 annual mean, respectively. Recently, Dong et al. (2019) evaluated BC emission inventories  
345 using GEOS-Chem and proposed that using the inventory compiled by Huang et al. (2015)  
346 for Russia, in which gas flaring accounted for 36 % of anthropogenic emissions, had no  
347 prominent impact on the simulation performance in Russia and the Arctic. They suggested  
348 that use of a new global inventory for BC emissions from natural gas flaring would improve  
349 the model performance (Huang and Fu, 2016). These results suggest that inclusion of BC  
350 emissions from gas flaring on the global scale is necessary for further BC simulations.

351 In Europe, a relatively high contribution of anthropogenic emissions to Arctic surface BC  
352 in January was made by Poland (50–55° N, 15–24° E, contributing 4 % of Arctic surface BC)  
353 because of relatively large emission fluxes in the region (Fig. S1a). Anthropogenic emissions  
354 from East China, especially those north of ~33° N (33–43° N, 109–126° E), contributed  
355 perceptibly (5 %) to Arctic surface BC.

356 In July, contributions from anthropogenic sources shrank to those from Yamalo-Nenets  
357 Autonomous Okrug and Komi Republic in Russia, and contributed a lower fraction (3 % of  
358 Arctic surface BC) (Fig. 6b). Few open biomass burning sources contributed in January (Fig.  
359 6c), but contributions from open biomass burning to Arctic surface BC in July can be clearly  
360 seen, mainly from the far east of Russia, Canada, and Alaska (Fig. 6d). Open biomass burning  
361 emissions from Kazakhstan, southwest Russia, southern Siberia, and northeast China also  
362 contributed to Arctic surface BC, although at relatively low strengths (Fig. 5d and Fig. S1d).  
363 However, the contributions from open biomass burning could be higher, as the MODIS  
364 burned area, the basis of GFED emission inventories, was underestimated for northern  
365 Eurasia by 16 % (Zhu et al., 2017). Evangeliou et al. (2016) estimated a relatively high  
366 transport efficiency of BC from open biomass burning emissions to the Arctic, which led to a  
367 high contribution, i.e., 60 %, from such sources to BC deposition in the Arctic in 2010. A  
368 recent study suggested that open fires burned in western Greenland in summer (31 July to  
369 21 August 2017) could potentially alter the Arctic air composition and foster glacier melting  
370 (Evangeliou et al., 2019). Although the footprint of Arctic surface BC showed a relatively  
371 weak sensitivity to areas such as forests and tundra, in the boreal regions, pollutants from  
372 boreal wildfires could have greater effects on the Arctic air composition in summer under  
373 future warming scenarios (Veira et al., 2016).

#### 374 **3.4 Sources of Arctic BC at high altitudes**

375 Arctic BC levels at high altitudes showed the highest levels in spring (March–April, 40.5–  
376 53.9 ng m<sup>-3</sup>), followed by those in late autumn to early winter (November–January, 36.5–  
377 40.0 ng m<sup>-3</sup>), and summer (July–August, 33.0–39.0 ng m<sup>-3</sup>) (Fig. 4c). The annual mean Arctic  
378 BC at high altitudes was estimated to be 35.2 ng m<sup>-3</sup>, which is ca. 73 % of those at the  
379 surface. Such a vertical profile is in accordance with those based on aircraft measurements  
380 over the High Canadian Arctic (Schulz et al., 2019). Similarly to the case for the surface,  
381 anthropogenic sources dominated by residential sectors, transport, industry and energy  
382 (excluding gas flaring), accounted for 94–100 % of Arctic BC at high altitudes in October–  
383 May (Figs. 4c, 5c). East Asia accounted for 34–65 % of the total BC in October–May (40 %  
384 annually). In comparison, using the Community Atmosphere Model version 5 driven by the  
385 NASA Modern Era Retrospective-Analysis for Research and Applications reanalysis data and  
386 the IPCC AR5 year 2000 BC emission inventory, H. Wang et al. (2014) found that East Asia  
387 accounted for 23% of BC burden in the Arctic for 1995–2005. In summer, open biomass  
388 burning in the boreal regions accounted for 40–72 % (57 % on average) of Arctic BC at high  
389 altitudes, similar to the source contributions to Arctic surface BC. Specifically, open biomass  
390 burning sources from Siberia accounted for 40–42 % of Arctic BC at high altitudes in July–  
391 August. Annually, anthropogenic sources and open biomass burning accounted for 83 % (in  
392 which residential sources accounted for 34%) and 17 %, respectively, of total Arctic BC at  
393 high altitudes (Figs. 4d, 5d).

394 Further investigations of geospatial contributions to Arctic BC at high altitudes in January  
395 and July provided more details regarding BC sources. In January, the main anthropogenic BC  
396 source in East Asia covered a wide range in China (Fig. 7a). Not only east and northeast  
397 China, but also southwest China (Sichuan and Guizhou provinces) were the major  
398 anthropogenic sources of Arctic BC at high altitudes. In July, anthropogenic sources made a

399 relatively weak contribution to Arctic BC at high altitudes. The regions that were sources of  
400 open biomass burning contributions to Arctic BC at high altitudes were mainly the far east of  
401 Siberia, Kazakhstan, central Canada, and Alaska, i.e., similar to the sources of Arctic surface  
402 BC. Unlike Arctic surface BC, for which the dominant source regions are at high latitudes in  
403 both winter and summer, Arctic BC at high altitudes mainly originates from mid-latitude  
404 regions (Figs. 6 and 7). In terms of transport pathways, air masses could be uplifted at low-  
405 to-mid latitudes and transported to the Arctic (Stohl, 2006). Further investigations are  
406 needed to obtain more details of the transport processes.

### 407 **3.5 Comparison of Flexpart and GEOS-Chem simulations of BC sources**

408 Data for BC sources simulated with Flexpart were compared with those obtained with  
409 GEOS-Chem (Ikeda et al., 2017), which is an Eulerian atmospheric transport model, using the  
410 same emission inventories. The simulated seasonal variations in Arctic BC levels and source  
411 contributions obtained with Flexpart agreed well with those obtained with GEOS-Chem (Fig.  
412 S3). The annual mean BC levels at the Arctic surface obtained by Flexpart and GEOS-Chem  
413 simulations were 48 and 70 ng m<sup>-3</sup>, respectively; the high-altitude values simulated by  
414 Flexpart and GEOS-Chem were 35 and 38 ng m<sup>-3</sup>, respectively. The magnitude difference  
415 between the BC levels at the Arctic surface could be related to meteorology. ECMWF ERA-  
416 Interim data were used as the input for the Flexpart simulation, whereas the GEOS-Chem  
417 simulation was driven by assimilated meteorological data from the Goddard Earth  
418 Observation System (GEOS-5).

419 The treatments of the BC removal processes could also lead to different simulation  
420 results, depending on the model. In terms of BC loss processes, dry and wet depositions  
421 were the removal pathways, depending on the particle size and density, in Flexpart. The  
422 treatment of meteorology, especially cloud water and precipitation, would therefore affect

423 the uncertainties of the simulations. In Flexpart version 10.1, BC particles are separately  
424 parameterized as ice nuclei for ice clouds, cloud condensation nuclei for liquid-water clouds,  
425 and 90 % as cloud condensation nuclei for mixed-phase clouds. The separation of mixed-  
426 phase clouds is realistic, as 77 % of in-cloud scavenging processes occurred in the mixed  
427 phase over a 90 day period starting from December 2006 (Grythe et al., 2017).

428 In GEOS-Chem simulations, the BC aging was parameterized based on the number  
429 concentration of OH radicals (Liu et al., 2011). The BC was assumed to be hydrophilic in  
430 liquid clouds ( $T \geq 258$  K) and hydrophobic when serving as ice nuclei in ice clouds ( $T < 258$  K)  
431 (Wang et al., 2011), with modifications because the scavenging rate of hydrophobic BC was  
432 reduced to 5 % of water-soluble aerosols for liquid clouds (Bourgeois and Bey, 2011). Such a  
433 treatment is expected to improve the simulation accuracy (Ikeda et al., 2017).

434 In Lagrangian models, the trajectories of particles are computed by following the  
435 movement of air masses with no numerical diffusion, although some artificial numerical  
436 errors could be generated from stochastic differential equations (Ramli and Esler, 2016). As  
437 a result, long-range transport processes can be well simulated (Stohl, 2006; Stohl et al.,  
438 2013). In comparison, Eulerian chemical transport models such as GEOS-Chem have the  
439 advantage of simulating non-linear processes on the global scale, which enables treatment  
440 of the BC aging processes (coating with soluble components) (Bey et al, 2001; Eastham et  
441 al., 2018). However, with GEOS-Chem, the capture of intercontinental pollution plumes is  
442 difficult because of numerical plume dissipation (Rastigejev et al., 2010). Nevertheless, the  
443 agreement between the Flexpart and GEO-Chem simulations of BC source contributions  
444 indicates improved reliability of evaluated source contributions to Arctic BC.

#### 445 **4 Conclusions**

446 The source contributions to Arctic BC were investigated by using a Flexpart (version 10.1)  
447 transport model that incorporated emission inventories. Flexpart-simulated BC data agreed  
448 well with observations at Arctic sites, i.e., Barrow, Alert, Zeppelin, and Tiksi. The source  
449 regions and source sectors of BC at the surface and high altitudes over a wide region in the  
450 Arctic north of 66° N were simulated. BC at the Arctic surface was sensitive to local  
451 emissions and those from nearby Nordic countries (>60° N). These results emphasize the  
452 role of anthropogenic emissions such as gas flaring and development of the Northern Sea  
453 Route in affecting air quality and climate change in the Arctic. Anthropogenic emissions in  
454 the northern regions of Russia were the main source (56 %) of Arctic surface BC annually. In  
455 contrast, BC in the Arctic at high altitudes was sensitive to mid-latitude emissions (30–60°  
456 N). Although they are geospatially far from the Arctic, anthropogenic emissions in East Asia  
457 made a notable (40 %) contribution to BC in the Arctic at high altitudes annually. Open  
458 biomass burning emissions, which were mainly from Siberia, Alaska, and Canada, were  
459 important in summer, contributing 56–85 % of BC at the Arctic surface, and 40–72 % at  
460 Arctic high altitudes. Future increases in wildfires as a result of global warming could  
461 therefore increase the air pollution level during the Arctic summer. This study clarifies the  
462 source regions and sectors of BC in the Arctic. This information is fundamental for  
463 understanding and tackling air pollution and climate change in the region.

464  
465 *Data Availability.* The data set for simulated footprint and BC source contributions is  
466 available on request to the corresponding author.

467  
468 *Author contributions.* CZ and YK designed the study. CZ, MT, and IP optimized the Flexpart  
469 model. CZ performed Flexpart model simulations, conducted analyses, and wrote the

470 manuscript. KI and HT provided data for GEOS-Chem simulations and site observations. All  
471 authors made comments that improved the paper.

472

473 *Competing interests.* The authors declare that they have no conflict of interest.

474

475 *Financial Support.* This study was supported by the Environmental Research and Technology  
476 Development Fund (2-1505) of the Ministry of the Environment, Japan.

477

478 *Acknowledgment.* We acknowledge staffs from the following university and agencies for BC  
479 observational data: Barrow and Tiksi sites are operated by National Oceanic and  
480 Atmospheric Administration; Zeppelin site is operated by Stockholm University; and Alert  
481 site is operated by Environment and Climate Change Canada. We are grateful to Chandra  
482 Mouli Pavuluri (Tianjin University) and an anonymous reviewer for the comments. We thank  
483 Helen McPherson, PhD, from Edanz Group ([www.edanzediting.com/ac](http://www.edanzediting.com/ac)) for editing a draft of  
484 this manuscript.

485

#### 486 **References**

487 AMAP Assessment 2015: Black carbon and ozone as Arctic climate forcers, Arctic Monitoring  
488 and Assessment Programme (AMAP), Oslo, Norway, 2015.

489 Bey, I., Jacob, D. J., Yantosca, R. M., Logan, J. A., Field, B. D., Fiore, A. M., Li, Q. B., Liu, H. G.  
490 Y., Mickley, L. J., and Schultz, M. G.: Global modeling of tropospheric chemistry with  
491 assimilated meteorology: Model description and evaluation, *J Geophys Res-Atmos*, 106,  
492 23073-23095, doi:10.1029/2001jd000807, 2001.

493 [Bond, T. C., Bhardwaj, E., Dong, R., Jogani, R., Jung, S. K., Ro-den, C., Streets, D. G., and](#)  
494 [Trautmann, N. M.: Historical emis- sions of black and organic carbon aerosol from energy-](#)  
495 [related combustion, 1850-2000, \*Glob Biogeochem Cy\*, 21, Gb2018,](#)  
496 [doi:10.1029/2006GB002840, 2007.](#)

- 497 [Bond, T. C., Streets, D. G., Yarber, K. F., Nelson, S. M., Woo, J. H., and Klimont, Z.: A](#)  
498 [technology-based global inventory of black and organic carbon emissions from](#)  
499 [combustion, \*J Geophys Res\*, 109, D14203, doi:10.1029/2003JD003697, 2004.](#)
- 500 Bourgeois, Q. and Bey, I.: Pollution transport efficiency toward the Arctic: sensitivity to  
501 aerosol scavenging and source regions, *J. Geophys. Res.*, 116, D08213,  
502 doi:10.1029/2010JD015096, 2011.
- 503 Brock, C. A., Cozic, J., Bahreini, R., Froyd, K. D., Middlebrook, A. M., McComiskey, A.,  
504 Brioude, J., Cooper, O. R., Stohl, A., Aikin, K. C., de Gouw, J. A., Fahey, D. W., Ferrare, R.  
505 A., Gao, R. S., Gore, W., Holloway, J. S., Hubler, G., Jefferson, A., Lack, D. A., Lance, S.,  
506 Moore, R. H., Murphy, D. M., Nenes, A., Novelli, P. C., Nowak, J. B., Ogren, J. A., Peischl, J.,  
507 Pierce, R. B., Pilewskie, P., Quinn, P. K., Ryerson, T. B., Schmidt, K. S., Schwarz, J. P.,  
508 Sodemann, H., Spackman, J. R., Stark, H., Thomson, D. S., Thornberry, T., Veres, P., Watts,  
509 L. A., Warneke, C., and Wollny, A. G.: Characteristics, sources, and transport of aerosols  
510 measured in spring 2008 during the aerosol, radiation, and cloud processes affecting  
511 Arctic Climate (ARCPAC) Project, *Atmospheric Chemistry and Physics*, 11, 2423-2453,  
512 doi:10.5194/acp-11-2423-2011, 2011.
- 513 Cohen, J., Screen, J. A., Furtado, J. C., Barlow, M., Whittleston, D., Coumou, D., Francis, J.,  
514 Dethloff, K., Entekhabi, D., Overland, J., and Jones, J.: Recent Arctic amplification and  
515 extreme mid-latitude weather, *Nature Geoscience*, 7, 627-637, doi:10.1038/Ngeo2234,  
516 2014.
- 517 [Cooke, W. F. and Wilson, J. J. N.: A global black carbon aerosol model, \*J. Geophys. Res.-\*](#)  
518 [Atmos., 101\(D14\), 19395-19409, 1996.](#)
- 519 Cozic, J., Verheggen, B., Mertes, S., Connolly, P., Bower, K., Petzold, A., Baltensperger, U.,  
520 and Weingartner, E.: Scavenging of black carbon in mixed phase clouds at the high alpine  
521 site Jungfraujoch, *Atmos. Chem. Phys.*, 7, 1797-1807, doi:10.5194/acp-7-1797-2007,  
522 2007.
- 523 Dong, X., Zhu, Q., Fu, J. S., Huang, K., Tan, J., and Tipton, M.: Evaluating recent updated black  
524 carbon emissions and revisiting the direct radiative forcing in Arctic, *Geophysical*  
525 *Research Letters*, 46, 3560-3570. doi:10.1029/2018GL081242, 2019.
- 526 Eastham, S. D., Long, M. S., Keller, C. A., Lundgren, E., Yantosca, R. M., Zhuang, J. W., Li, C.,  
527 Lee, C. J., Yannetti, M., Auer, B. M., Clune, T. L., Kouatchou, J., Putman, W. M., Thompson,  
528 M. A., Trayanov, A. L., Molod, A. M., Martin, R. V., and Jacob, D. J.: GEOS-Chem High



- 529 Performance (GCHP v11-02c): a next-generation implementation of the GEOS-Chem  
530 chemical transport model for massively parallel applications, *Geosci Model Dev*, 11,  
531 2941-2953, doi:10.5194/gmd-11-2941-2018, 2018.
- 532 Eckhardt, S., Quennehen, B., Olivie, D. J. L., Berntsen, T. K., Cherian, R., Christensen, J. H.,  
533 Collins, W., Crepinsek, S., Daskalakis, N., Flanner, M., Herber, A., Heyes, C., Hodnebrog,  
534 O., Huang, L., Kanakidou, M., Klimont, Z., Langner, J., Law, K. S., Lund, M. T., Mahmood,  
535 R., Massling, A., Myriokefalitakis, S., Nielsen, I. E., Nojgaard, J. K., Quaas, J., Quinn, P. K.,  
536 Raut, J. C., Rumbold, S. T., Schulz, M., Sharma, S., Skeie, R. B., Skov, H., Uttal, T., von  
537 Salzen, K., and Stohl, A.: Current model capabilities for simulating black carbon and  
538 sulfate concentrations in the Arctic atmosphere: a multi-model evaluation using a  
539 comprehensive measurement data set, *Atmospheric Chemistry and Physics*, 15, 9413-  
540 9433, doi:10.5194/acp-15-9413-2015, 2015.
- 541 Evangeliou, N., Balkanski, Y., Hao, W. M., Petkov, A., Silverstein, R. P., Corley, R., Nordgren,  
542 B. L., Urbanski, S. P., Eckhardt, S., Stohl, A., Tunved, P., Crepinsek, S., Jefferson, A.,  
543 Sharma, S., Nojgaard, J. K., and Skov, H.: Wildfires in northern Eurasia affect the budget of  
544 black carbon in the Arctic - a 12-year retrospective synopsis (2002-2013), *Atmospheric  
545 Chemistry and Physics*, 16, 7587-7604, doi:10.5194/acp-16-7587-2016, 2016.
- 546 Evangeliou, N., Kylling, A., Eckhardt, S., Myroniuk, V., Stebel, K., Paugam, R., Zibtsev, S., and  
547 Stohl, A.: Open fires in Greenland in summer 2017: transport, deposition and radiative  
548 effects of BC, OC and BrC emissions, *Atmospheric Chemistry and Physics*, 19, 1393-1411,  
549 doi:10.5194/acp-19-1393-2019, 2019.
- 550 Filimonova, I. V., Komarova, A. V., Eder, L. V., and Provornaya, I. V.: State instruments for the  
551 development stimulation of Arctic resources regions, *IOP Conference Series: Earth and  
552 Environmental Science*, 193, 012069, doi:10.1088/1755-1315/193/1/012069, 2018.
- 553 Garrett, T. J., Brattstrom, S., Sharma, S., Worthy, D. E. J., and Novelli, P.: The role of  
554 scavenging in the seasonal transport of black carbon and sulfate to the Arctic,  
555 *Geophysical Research Letters*, 38, L16805, doi:10.1029/2011gl048221, 2011.
- 556 Grythe, H., Kristiansen, N. I., Zwaafink, C. D. G., Eckhardt, S., Strom, J., Tunved, P., Krejci, R.,  
557 and Stohl, A.: A new aerosol wet removal scheme for the Lagrangian particle model  
558 FLEXPART v10, *Geosci Model Dev*, 10, 1447-1466, doi:10.5194/gmd-10-1447-2017, 2017.

- 559 Hegg, D. A., Clarke, A. D., Doherty, S. J., and Ström, J.: Measurements of black carbon  
560 aerosol washout ratio on Svalbard, *Tellus B*, 63, 891–900, doi:10.1111/j.1600-  
561 0889.2011.00577.x, 2011.
- 562 Hertel, O., Christensen, J. Runge, E. H., Asman, W. A. H., Berkowicz, R., Hovmand, M. F., and  
563 Hov, O.: Development and testing of a new variable scale air pollution model – ACDEP,  
564 *Atmos. Environ.*, 29, 1267–1290, 1995.
- 565 Hirdman, D., Burkhardt, J. F., Sodemann, H., Eckhardt, S., Jefferson, A., Quinn, P. K., Sharma,  
566 S., Strom, J., and Stohl, A.: Long-term trends of black carbon and sulphate aerosol in the  
567 Arctic: changes in atmospheric transport and source region emissions, *Atmospheric*  
568 *Chemistry and Physics*, 10, 9351-9368, doi:10.5194/acp-10-9351-2010, 2010.
- 569 Huang, K., and Fu, J. S.: A global gas flaring black carbon emission rate dataset from 1994 to  
570 2012, *Scientific Data*, 3, 160104. doi:10.1038/sdata.2016.104, 2016.
- 571 Huang, K., Fu, J. S., Prikhodko, V. Y., Storey, J. M., Romanov, A., Hodson, E. L., Cresko, J.,  
572 Morozova, I., Ignatieva, Y., and Cabaniss, J.: Russian anthropogenic black carbon:  
573 Emission reconstruction and Arctic black carbon simulation, *J Geophys Res-Atmos*, 120,  
574 11306-11333, doi:10.1002/2015jd023358, 2015.
- 575 Ikeda, K., Tanimoto, H., Sugita, T., Akiyoshi, H., Kanaya, Y., Zhu, C. M., and Taketani, F.:  
576 Tagged tracer simulations of black carbon in the Arctic: transport, source contributions,  
577 and budget, *Atmospheric Chemistry and Physics*, 17, 10515-10533, doi:10.5194/acp-17-  
578 10515-2017, 2017.
- 579 Janssens-Maenhout, G., Crippa, M., Guizzardi, D., Dentener, F., Muntean, M., Pouliot, G.,  
580 Keating, T., Zhang, Q., Kurokawa, J., Wankmüller, R., Denier van der Gon, H., Kuenen, J. J.  
581 P., Klimont, Z., Frost, G., Darras, S., Koffi, B., and Li, M.: HTAP\_v2.2: a mosaic of regional  
582 and global emission grid maps for 2008 and 2010 to study hemispheric transport of air  
583 pollution, *Atmos. Chem. Phys.*, 15, 11411–11432, doi:10.5194/acp-15-11411-2015, 2015.
- 584 Keegan, K. M., Albert, M. R., McConnell, J. R., and Baker, I.: Climate change and forest fires  
585 synergistically drive widespread melt events of the Greenland Ice Sheet, *P Natl Acad Sci*  
586 *USA*, 111, 7964-7967, doi:10.1073/pnas.1405397111, 2014.
- 587 Kipling, Z., Stier, P., Schwarz, J. P., Perring, A. E., Spackman, J. R., Mann, G. W., Johnson, C.  
588 E., and Telford, P. J.: Constraints on aerosol processes in climate models from vertically-  
589 resolved aircraft observations of black carbon, *Atmos. Chem. Phys.*, 13, 5969–5986,  
590 doi:10.5194/acp-13-5969-2013, 2013.

- 591 Kirchstetter, T. W., Novakov, T., and Hobbs, P. V.: Evidence that the spectral dependence of  
 592 light absorption by aerosols is affected by organic carbon, *J Geophys Res-Atmos*, 109,  
 593 D21208, doi:10.1029/2004jd004999, 2004.
- 594 Klimont, Z., Kupiainen, K., Heyes, C., Purohit, P., Cofala, J., Rafaj, P., Borken-Kleefeld, J., and  
 595 Schöpp, W.: Global anthropogenic emissions of particulate matter including black carbon,  
 596 *Atmos. Chem. Phys.*, 17, 8681–8723, doi:10.5194/acp-17-8681-2017, 2017.
- 597 Klonecki, A., Hess, P., Emmons, L., Smith, L., Orlando, J., and Blake, D.: Seasonal changes in  
 598 the transport of pollutants into the Arctic troposphere-model study, *J Geophys Res-*  
 599 *Atmos*, 108, 8367, doi:10.1029/2002jd002199, 2003.
- 600 Koch, D., and Hansen, J.: Distant origins of Arctic black carbon: A Goddard Institute for Space  
 601 Studies ModelE experiment, *J Geophys Res-Atmos*, 110, D04204,  
 602 doi:10.1029/2004jd005296, 2005.
- 603 Koch, D., Schmidt, G. A., and Field, C. V.: Sulfur, sea salt, and radionuclide aerosols in GISS  
 604 ModelE, *J. Geophys. Res.*, 111, D06206, doi:10.1029/2004jd005550, 2006.
- 605 Lack, D. A., and Langridge, J. M.: On the attribution of black and brown carbon light  
 606 absorption using the Angstrom exponent, *Atmospheric Chemistry and Physics*, 13,  
 607 10535–10543, doi:10.5194/acp-13-10535-2013, 2013.
- 608 Law, K. S., and Stohl, A.: Arctic air pollution: Origins and impacts, *Science*, 315, 1537–1540,  
 609 doi:10.1126/science.1137695, 2007.
- 610 Liu, J., Fan, S., Horowitz, L. W., and Levy II, H.: Evaluation of factors controlling long-range  
 611 transport of black carbon to the Arctic, *J. Geophys. Res.*, 116, D00A14,  
 612 doi:10.1029/2010JD015145, 2011.
- 613 Liu, D., Quennehen, B., Darbyshire, E., Allan, J. D., Williams, P. I., Taylor, J. W., Bauguitte, S. J.  
 614 B., Flynn, M. J., Lowe, D., Gallagher, M. W., Bower, K. N., Choulaton, T. W., and Coe, H.:  
 615 The importance of Asia as a source of black carbon to the European Arctic during  
 616 springtime 2013, *Atmospheric Chemistry and Physics*, 15, 11537–11555, doi:10.5194/acp-  
 617 15-11537-2015, 2015.
- 618 [Ma, P.-L., Gattiker, J. R., Liu, X., and Rasch, P. J.: A novel approach for determining source-](#)  
 619 [receptor relationships in model simulations: a case study of black carbon transport in](#)  
 620 [northern hemisphere winter, \*Environ Res Lett\*, 8, 024042, doi:10.1088/1748-](#)  
 621 [9326/8/2/024042, 2013,](#)

**Deleted:** Ma, P.-L., Rasch, P. J., Wang, H., Zhang, K.,  
 Easter, R. C., Tilmes, S., Fast, J. D., Liu, X., Yoon, J.-H., and  
 Lamarque, J.-F.: The role of circulation features on black  
 carbon transport into the Arctic in the Community  
 Atmosphere Model version 5 (CAM5), *J. Geophys. Res.-*  
*Atmos.*, 118, 4657–4669, doi:10.1002/jgrd.50411, 2013

- 628 McMahon, T. A. and Denison, P. J.: Empirical atmospheric deposition parameters – a survey,  
629 *Atmos. Environ.*, 13, 571–585, doi:10.1016/0004-6981(79)90186-0, 1979.
- 630 Najafi, M. R., Zwiers, F. W., and Gillett, N. P.: Attribution of Arctic temperature change to  
631 greenhouse-gas and aerosol influences, *Nature Climate Change*, 5, 246-249,  
632 doi:10.1038/Nclimate2524, 2015.
- 633 Park, R. J., Jacob, D. J., Palmer, P. I., Clarke, A. D., Weber, R. J., Zondlo, M. A., Eisele, F. L.,  
634 Bandy, A. R., Thornton, D. C., Sachse, G. W., and Bond, T. C.: Export efficiency of black  
635 carbon aerosol in continental outflow: Global implications, *J Geophys Res-Atmos*, 110,  
636 D11205, doi:10.1029/2004jd005432, 2005.
- 637 Qi, L., Li, Q. B., Henze, D. K., Tseng, H. L., and He, C. L.: Sources of springtime surface black  
638 carbon in the Arctic: an adjoint analysis for April 2008, *Atmospheric Chemistry and  
639 Physics*, 17, 9697–9716, doi:10.5194/acp-17-9697-2017, 2017.
- 640 Quinn, P. K., Bates, T. S., Baum, E., Doubleday, N., Fiore, A. M., Flanner, M., Fridlind, A.,  
641 Garrett, T. J., Koch, D., Menon, S., Shindell, D., Stohl, A., and Warren, S. G.: Short-lived  
642 pollutants in the Arctic: their climate impact and possible mitigation strategies,  
643 *Atmospheric Chemistry and Physics*, 8, 1723–1735, doi:10.5194/acp-8-1723-2008, 2008.
- 644 Ramli, H. M. and Esler, J. G.: Quantitative evaluation of numerical integration schemes for  
645 Lagrangian particle dispersion models, *Geosci. Model Dev.*, 9, 2441–2457,  
646 doi:10.5194/gmd-9-2441-2016, 2016.
- 647 Rastigejev, Y., Park, R., Brenner, M., and Jacob, D.: Resolving intercontinental pollution  
648 plumes in global models of atmospheric transport, *J. Geophys. Res.*, 115, D02302,  
649 doi:10.1029/2009JD012568, 2010.
- 650 Roiger, A., Thomas, J. L., Schlager, H., Law, K. S., Kim, J., Schafner, A., Weinzierl, B.,  
651 Dahlokter, F., Krisch, I., Marelle, L., Minikin, A., Raut, J. C., Reiter, A., Rose, M., Scheibe,  
652 M., Stock, P., Baumann, R., Bouapar, I., Clerbaux, C., George, M., Onishi, I., and Flemming,  
653 J.: Quantifying emerging local anthropogenic emissions in the Arctic region: The ACCESS  
654 aircraft campaign experiment, *B. Am. Meteorol. Soc.*, 96, 441–460, doi:10.1175/Bams-D-  
655 13-00169.1, 2015.
- 656 Sand, M., Berntsen, T. K., von Salzen, K., Flanner, M. G., Langner, J., and Victor, D. G.:  
657 Response of Arctic temperature to changes in emissions of short-lived climate forcers,  
658 *Nature Climate Change*, 6, 286-289, doi:10.1038/Nclimate2880, 2016.

- 659 Schacht, J., Heinold, B., Quaas, J., Backman, J., Cherian, R., Ehrlich, A., Herber, A., Huang, W.  
660 T. K., Kondo, Y., Massling, A., Sinha, P. R., Weinzierl, B., Zanatta, M., and Tegen, I.: The  
661 importance of the representation of air pollution emissions for the modeled distribution  
662 and radiative effects of black carbon in the Arctic, *Atmos. Chem. Phys.*, **19**, 11159–11183,  
663 doi:10.5194/acp-19-11159-2019, 2019.
- 664 Schmale, J., Arnold, S. R., Law, K. S., Thorp, T., Anenberg, S., Simpson, W. R., Mao, J., and  
665 Pratt, K. A.: Local Arctic Air Pollution: A Neglected but Serious Problem, *Earths Future*, **6**,  
666 1385–1412, doi:10.1029/2018ef000952, 2018.
- 667 Schulz, H., Zanatta, M., Bozem, H., Leaitch, W. R., Herber, A. B., Burkart, J., Willis, M. D.,  
668 Kunkel, D., Hoor, P. M., Abbatt, J. P. D., and Gerdes, R.: High Arctic aircraft measurements  
669 characterising black carbon vertical variability in spring and summer, *Atmospheric*  
670 *Chemistry and Physics*, **19**, 2361–2384, doi:10.5194/acp-19-2361-2019, 2019.
- 671 Sharma, S., Leaitch, W. R., Huang, L., Veber, D., Kolonjari, F., Zhang, W., Hanna, S. J.,  
672 Bertram, A. K., and Ogren, J. A.: An evaluation of three methods for measuring black  
673 carbon in Alert, Canada, *Atmospheric Chemistry and Physics*, **17**, 15225–15243,  
674 doi:10.5194/acp-17-15225-2017, 2017.
- 675 Shaw, G. E.: The arctic haze phenomenon, *B Am Meteorol Soc*, **76**, 2403–2413, 1995.
- 676 Shen, Z. Y., Ming, Y., Horowitz, L. W., Ramaswamy, V., and Lin, M. Y.: On the seasonality of  
677 Arctic black carbon, *J. Climate*, **30**, 4429–4441, doi:10.1175/Jcli-D-16-0580.1, 2017.
- 678 Shindell, D. T., Chin, M., Dentener, F., Doherty, R. M., Faluvegi, G., Fiore, A. M., Hess, P.,  
679 Koch, D. M., MacKenzie, I. A., Sanderson, M. G., Schultz, M. G., Schulz, M., Stevenson, D.  
680 S., Teich, H., Textor, C., Wild, O., Bergmann, D. J., Bey, I., Bian, H., Cuvelier, C., Duncan, B.  
681 N., Folberth, G., Horowitz, L. W., Jonson, J., Kaminski, J. W., Marmer, E., Park, R., Pringle,  
682 K. J., Schroeder, S., Szopa, S., Takemura, T., Zeng, G., Keating, T. J., and Zuber, A.: A multi-  
683 model assessment of pollution transport to the Arctic, *Atmos. Chem. Phys.*, **8**, 5353–5372,  
684 doi:10.5194/acp-8-5353-2008, 2008.
- 685 Sinha, P. R., Kondo, Y., Koike, M., Ogren, J. A., Jefferson, A., Barrett, T. E., Sheesley, R. J.,  
686 Ohata, S., Moteki, N., Coe, H., Liu, D., Irwin, M., Tunved, P., Quinn, P. K., and Zhao, Y.:  
687 Evaluation of ground-based black carbon measurements by filter-based photometers at  
688 two Arctic sites, *J Geophys Res-Atmos*, **122**, 3544–3572, doi:10.1002/2016jd025843,  
689 2017.

- 690 Stohl, A., Forster, C., Frank, A., Seibert, P., and Wotawa, G.: Technical note: The Lagrangian  
691 particle dispersion model FLEXPART version 6.2, *Atmos. Chem. Phys.*, 5, 2461–2474,  
692 doi:10.5194/acp-5-2461-2005, 2005.
- 693 Stohl, A.: Characteristics of atmospheric transport into the Arctic troposphere, *J Geophys*  
694 *Res-Atmos*, 111, D11306, doi:10.1029/2005jd006888, 2006.
- 695 Stohl, A., Hittenberger, M., and Wotawa, G.: Validation of the Lagrangian particle dispersion  
696 model FLEXPART against large-scale tracer experiment data, *Atmos Environ*, 32, 4245-  
697 4264, doi:10.1016/S1352-2310(98)00184-8, 1998.
- 698 Stohl, A., Klimont, Z., Eckhardt, S., Kupiainen, K., Shevchenko, V. P., Kopeikin, V. M., and  
699 Novigatsky, A. N.: Black carbon in the Arctic: the underestimated role of gas flaring and  
700 residential combustion emissions, *Atmospheric Chemistry and Physics*, 13, 8833-8855,  
701 doi:10.5194/acp-13-8833-2013, 2013.
- 702 Taketani, F., Miyakawa, T., Takashima, H., Komazaki, Y., Pan, X., Kanaya, Y., and Inoue, J.:  
703 Shipborne observations of atmospheric black carbon aerosol particles over the Arctic  
704 Ocean, Bering Sea, and North Pacific Ocean during September 2014, *J Geophys Res-*  
705 *Atmos*, 121, 1914-1921, doi:10.1002/2015jd023648, 2016.
- 706 Tietze, K., Riedi, J., Stohl, A., and Garrett, T. J.: Space-based evaluation of interactions  
707 between aerosols and low-level Arctic clouds during the Spring and Summer of 2008,  
708 *Atmospheric Chemistry and Physics*, 11, 3359-3373, doi:10.5194/acp-11-3359-2011,  
709 2011.
- 710 Tilling, R. L., Ridout, A., Shepherd, A., and Wingham, D. J.: Increased Arctic sea ice volume  
711 after anomalously low melting in 2013, *Nature Geoscience*, 8, 643-646,  
712 doi:10.1038/Ngeo2489, 2015.
- 713 Tørseth, K., Aas, W., Breivik, K., Fjærraa, A. M., Fiebig, M., Hjellbrekke, A. G., Lund Myhre, C.,  
714 Solberg, S., and Yttri, K. E.: Introduction to the European Monitoring and Evaluation  
715 Programme (EMEP) and observed atmospheric composition change during 1972–2009,  
716 *Atmos. Chem. Phys.*, 12, 5447–5481, doi:10.5194/acp-12-5447-2012, 2012.
- 717 Trusel, L. D., Das, S. B., Osman, M. B., Evans, M. J., Smith, B., Fettweis, X., McConnell, J. R.,  
718 Noel, B. P. Y., and van den Broeke, M. R.: Nonlinear rise in Greenland runoff in response  
719 to post-industrial Arctic warming, *Nature*, 564, 104-108, doi:10.1038/s41586-018-0752-4,  
720 2018.

- 721 van der Werf, G. R., Randerson, J. T., Giglio, L., Collatz, G. J., Mu, M., Kasibhatla, P. S.,  
722 Morton, D. C., DeFries, R. S., Jin, Y., and van Leeuwen, T. T.: Global fire emissions and the  
723 contribution of deforestation, savanna, forest, agricultural, and peat fires (1997–2009),  
724 Atmospheric Chemistry and Physics, 10, 11707–11735, doi:10.5194/acp-10-11707-2010,  
725 2010.
- 726 Veira, A., Lasslop, G., and Kloster, S.: Wildfires in a warmer climate: Emission fluxes,  
727 emission heights, and black carbon concentrations in 2090–2099, J Geophys Res-Atmos,  
728 121, 3195–3223, doi:10.1002/2015jd024142, 2016.
- 729 [Wang, H., Easter, R. C., Rasch, P. J., Wang, M., Liu, X., Ghan, S. J., Qian, Y., Yoon, J. H., Ma, P.](#)  
730 [L., and Vinoj, V.: Sensitivity of remote aerosol distributions to representation of cloud–](#)  
731 [aerosol interactions in a global climate model, Geosci. Model Dev., 6, 765–782,](#)  
732 [doi:10.5194/gmd-6-765-2013, 2013.](#)
- 733 Wang, H., Rasch, P. J., Easter, R. C., Singh, B., Zhang, R., Ma, P. L., Qian, Y., and Beagley, N.:  
734 Using an explicit emission tag- ging method in global modeling of source-receptor  
735 relationships for black carbon in the Arctic: Variations, Sources and Trans- port pathways,  
736 J. Geophys. Res.-Atmos., 119, 12888–12909, doi:10.1002/2014JD022297, 2014.
- 737 Wang, Q., Jacob, D. J., Fisher, J. A., Mao, J., Leibensperger, E. M., Carouge, C. C., Le Sager, P.,  
738 Kondo, Y., Jimenez, J. L., Cubison, M. J., and Doherty, S. J.: Sources of carbonaceous  
739 aerosols and deposited black carbon in the Arctic in winter-spring: implications for  
740 radiative forcing, Atmos. Chem. Phys., 11, 12453– 12473, doi:10.5194/acp-11-12453-  
741 2011, 2011.
- 742 Wang, Q., Jacob, D. J., Spackman, J. R., Perring, A. E., Schwarz, J. P., Moteki, N., Marais, E. A.,  
743 Ge, C., Wang, J., and Barrett, S. R. H.: Global budget and radiative forcing of black carbon  
744 aerosol: constraints from pole-to-pole (HIPPO) observations across the Pacific, J.  
745 Geophys. Res. Atmos., 119, 195–206, doi:10.1002/2013JD020824, 2014.
- 746 Winiger, P., Andersson, A., Eckhardt, S., Stohl, A., and Gustafsson, O.: The sources of  
747 atmospheric black carbon at a European gateway to the Arctic, Nat Commun, 7, 12776,  
748 doi:10.1038/ncomms12776, 2016.
- 749 Winiger, P., Barrett, T. E., Sheesley, R. J., Huang, L., Sharma, S., Barrie, L. A., Yttri, K. E.,  
750 Evangeliou, N., Eckhardt, S., Stohl, A., Klimont, Z., Heyes, C., Semiletov, I. P., Dudarev, O.  
751 V., Charkin, A., Shakhova, N., Holmstrand, H., Andersson, A., and Gustafsson, O.: Source

- 752 apportionment of circum-Arctic atmospheric black carbon from isotopes and modeling,  
753 *Sci Adv*, 5, eaau8052, doi:10.1126/sciadv.aau8052, 2019.
- 754 Xu, J. W., Martin, R. V., Morrow, A., Sharma, S., Huang, L., Leaitch, W. R., Burkart, J., Schulz,  
755 H., Zanatta, M., Willis, M. D., Henze, D. K., Lee, C. J., Herber, A. B., and Abbatt, J. P. D.:  
756 Source attribution of Arctic black carbon constrained by aircraft and surface  
757 measurements, *Atmospheric Chemistry and Physics*, 17, 11971-11989, doi:10.5194/acp-  
758 17-11971-2017, 2017.
- 759 Yang, Y., Wang, H., Smith, S. J., Easter, R. C., and Rasch, P. J.: Sulfate aerosol in the Arctic:  
760 Source attribution and radiative forcing, *J. Geophys. Res. Atmos.*, 123, 1899–1918,  
761 doi:10.1002/2017JD027298, 2018.
- 762 Yang, Y., Smith, S. J., Wang, H., Mills, C. M., and Rasch, P. J.: Variability, timescales, and  
763 nonlinearity in climate responses to black carbon emissions, *Atmospheric Chemistry and*  
764 *Physics*, 19, 2405–2420, doi:10.5194/acp-19-2405-2019, 2019.
- 765 Yu, K., Keller, C. A., Jacob, D. J., Molod, A. M., Eastham, S. D., and Long, M. S.: Errors and  
766 improvements in the use of archived meteorological data for chemical transport  
767 modeling: an analysis using GEOS-Chem v11-01 driven by GEOS-5 meteorology, *Geosci*  
768 *Model Dev*, 11, 305-319, doi:10.5194/gmd-11-305-2018, 2018.
- 769 [Zhang, K., O'Donnell, D., Kazil, J., Stier, P., Kinne, S., Lohmann, U., Ferrachat, S., Croft, B.,](#)  
770 [Quaas, J., Wan, H., Rast, S., and Feichter, J.: The global aerosol-climate model ECHAM-](#)  
771 [HAM, version 2: sensitivity to improvements in process representations, \*Atmos. Chem.\*](#)  
772 [Phys.](#), 12, 8911–8949, doi:10.5194/acp-12-8911-2012, 2012.
- 773 [Zhang, Q., Streets, D. G., Carmichael, G. R., He, K. B., Huo, H., Kannari, A., Klimont, Z., Park, J.](#)  
774 [S., Reddy, S., Fu, J. S., Chen, D., Duan, L., Lei, Y., Wang, L. T., and Yao, Z. L.: Asian](#)  
775 [emissions in 2006 for the NASA INTEX-B mission, \*Atmos Chem Phys\*](#), 9, 5131–5153,  
776 [doi:10.5194/acp-9-5131-2009, 2009.](#)
- 777 Zhu, C., Kobayashi, H., Kanaya, Y., and Saito, M.: Size-dependent validation of MODIS  
778 MCD64A1 burned area over six vegetation types in boreal Eurasia: Large underestimation  
779 in croplands, *Scientific reports*, 7, 4181, doi:10.1038/s41598-017-03739-0, 2017.

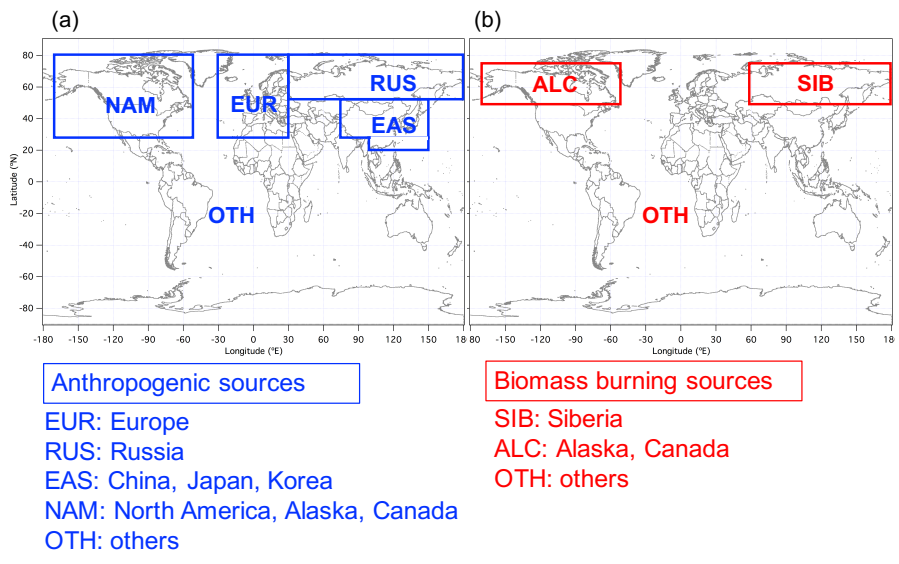


Table 1. Comparison of BC source contributions in the Arctic surface

Model and versions	Model type	Wet-deposition	Grid resolution	Meteorology	Emissions	Domain/Sites	Year/season	Major source regions/sector
Flexpart-WRF 6.2	Lagrangian	Stohl et al. (2005)	unspecified	WRF forecast	ECLIPSE, FINN	continental Norway and Svalbard	spring 2013	Asian anthropogenic
Flexpart 6.2	Lagrangian	Stohl et al. (2005)	1° × 1°	ECMWF operational	Unspecified (BC sensitivities were calculated)	Alert, Barrow, Zeppelin	1989-2009	Northern Eurasia
Flexpart 6.2	Lagrangian	Stohl et al. (2005)	1° × 1°	ECMWF operational	ECLIPSE4(GAINS), GFED3	Arctic (north of 66°N)	2008-2010	Flaring (42%), residential (>20%)
Flexpart 9.2	Lagrangian	Stohl et al. (2005)	1° × 1°	ECMWF operational	ECLIPSE5(GAINS), GFED4.1	Arctic (north of 66.7°N)	2011-2015	Residential and open burning (39%)
Flexpart 10.1	Lagrangian	Grythe et al. (2017)	1° × 1°	ECMWF operational	HTAP2, GFED3, Huang et al. (2015) for Russia flaring	Arctic (north of 66°N)	2010	Flaring (36%), open burning (18%), residential (15%), others (31%)
GEOS-Chem 9.02	CTM	Wang et al. (2011)	2° × 2.5°	GEOS-5	HTAP2, GFED3, Huang et al. (2015) for Russia flaring	Arctic (north of 66°N)	2007-2011	Russia (62%)
GEOS-Chem	CTM	Wang et al. (2011)	2° × 2.5°	GEOS-5	Bond et al. (2004), Zhang et al. (2009), GFED3	Alert, Barrow, Zeppelin	April 2008	Asian anthropogenic (35–45%), Siberian biomass burning (46–64%)

GEOS-Chem	CTM	Wang et al. (2011)	2° × 2.5°	GEOS-5	Bond et al. (2007), FLAMBE	North America Arctic	April 2008	Open fire (50%)	Wang et al. (2011)
GEOS-Chem10.01	CTM	Wang et al. (2011)	2° × 2.5°	GEOS-5	HTAP2, ECLIPSE5, GFED4	Alert, Barrow, Zeppelin, Arctic (north of 66.5°N)	2009-2011	Northern Asian anthropogenic (40–45%) in winter-spring	Xu et al. (2017)
<u>CAM5</u>	<u>GCM</u>	<u>Wang et al. (2013)</u>	<u>1.9° × 2.5°</u>	<u>MERRA</u>	<u>IPCC AR5</u>	<u>Arctic (north of 66.5°N)</u>	<u>1996-2005</u>	<u>Northern Europe in winter, Northern Asia in summer</u>	<u>Wang et al. (2014)</u>
<u>CAM5</u>	<u>GCM</u>	<u>Wang et al. (2013)</u>	<u>1.9° × 2.5°</u>	<u>Free running CAM5, ERA-Interim</u>	<u>POLARCAT-POLMIP</u>	<u>Arctic (north of ~66°N)</u>	<u>Winter 2008</u>	<u>Asia</u>	<u>Ma et al. (2013)</u>
<u>ECHAM-HAM</u>	<u>GCM</u>	<u>Zhang et al. (2012)</u>	<u>1.8° × 1.8°</u>	<u>ERA-Interim</u>	<u>ECLIPSE5, and Huang et al. (2015) for anthropogenic BC in Russia (default), GFES, and comparison with ACCMIP</u>	<u>Various sites and aircraft campaigns, Arctic (north of 60°N)</u>	<u>2005–2015</u>	<u>Northern Asia, Northern Europe, Russian gas flaring region (with default emission)</u>	<u>Schacht et al. (2019)</u>
GISS ModelE	GCM	Koch et al. (2006)	4° × 5°	Internal	Bond et al. (2004), Cooke and Wilson (1996)	Arctic (north of ~60°N)	Annual general	South Asia	Koch and Hansen (2005)

Deleted: N-

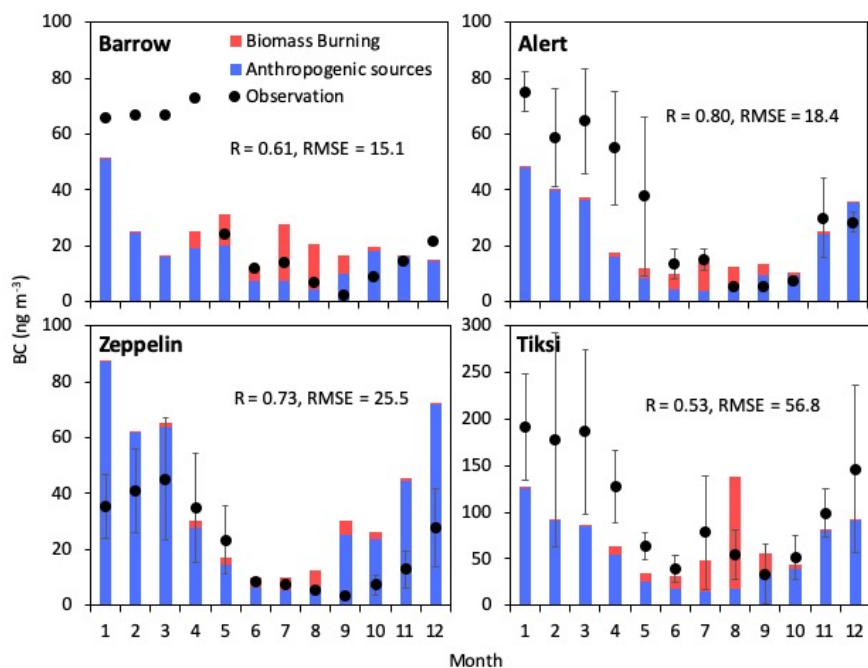


782

783 Figure 1. Regional separation for quantification of BC in the Arctic from (a) anthropogenic and

784 (b) open biomass burning sources.

785



786

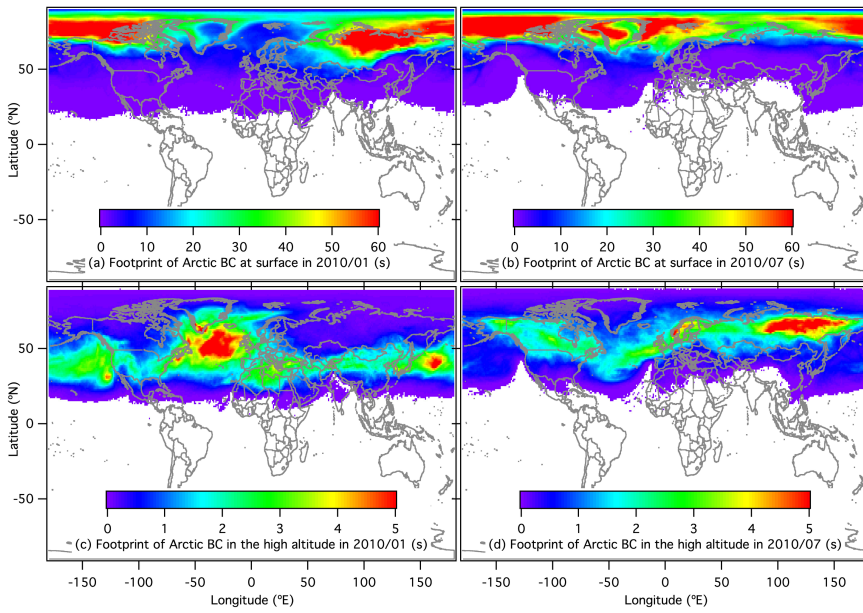
787 Figure 2. Observed (filled circles) and modeled (bars) seasonal variations in BC mass

788 concentrations at Arctic sites. Contributions from anthropogenic sources (blue) and open

789 biomass burning (red) in each month are shown. Monthly averages of observed (filled circles)

790 and simulated (bars) BC were conducted for 2007–2011 at Alert, Canada ( $62.3^\circ \text{ W}$ ,  $82.5^\circ \text{ N}$ ),791 and Zeppelin, Norway ( $11.9^\circ \text{ E}$ ,  $78.9^\circ \text{ N}$ ), for 2009 at Barrow, USA ( $156.6^\circ \text{ W}$ ,  $71.3^\circ \text{ N}$ ), and for792 2010–2014 at Tiksi, Russia ( $128.9^\circ \text{ E}$ ,  $71.6^\circ \text{ N}$ ). *R* and RMSE indicate correlation coefficient and793 root-mean-square error ( $\text{ng m}^{-3}$ ), respectively.

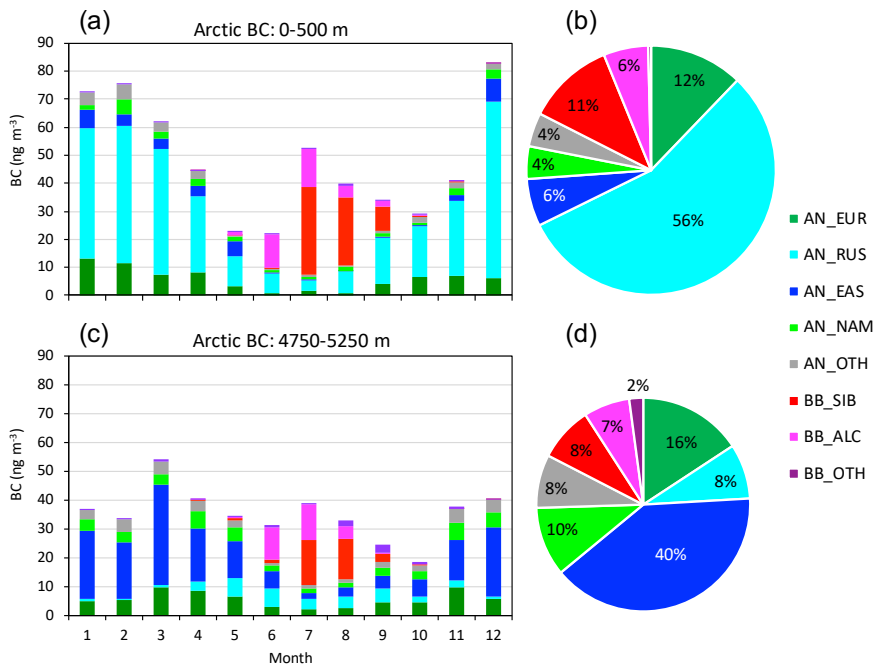
794



795

796 Figure 3. Footprints of Arctic BC shown as retention time(s) of (a) BC at surface (0–500 m) in  
797 January 2010, (b) BC at surface in July 2010, (c) BC at high altitudes (4750–5250 m) in January  
798 2010, and (d) BC at high altitudes in July 2010.

799



800

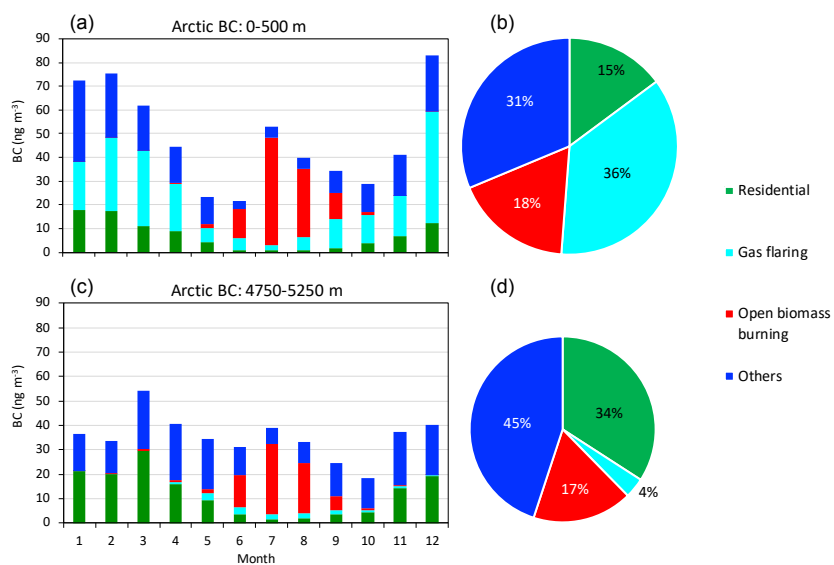
801 Figure 4. Contributions of anthropogenic sources (prefixed "AN\_" in the legend) and open

802 biomass burning ("BB\_") from each region to (a) seasonal variations in Arctic surface BC, (b)

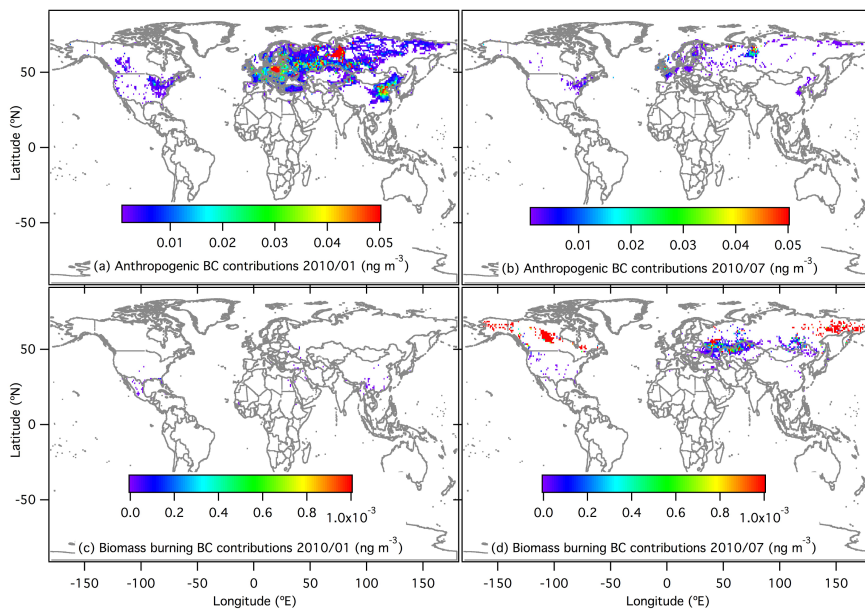
803 annual mean Arctic surface BC, (c) seasonal variations in Arctic BC at high altitudes, and (d)

804 annual mean of Arctic BC at high altitudes.

805



806  
 807 Figure 5. Sectorial contributions from residential combustion (including fossil fuel and biofuel  
 808 combustions), gas flaring, open biomass burning and others (energy other than gas flaring,  
 809 industry and transport) to (a) seasonal variations in Arctic surface BC, (b) annual mean Arctic  
 810 surface BC, (c) seasonal variations in Arctic BC at high altitudes, and (d) annual mean of Arctic  
 811 BC at high altitudes.  
 812

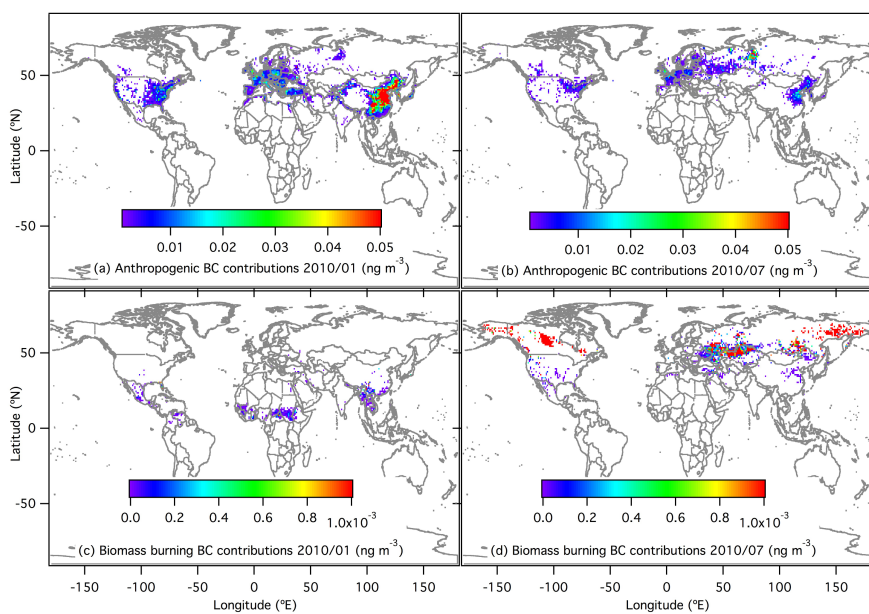


813

814 Figure 6. Spatial distributions of contributions to Arctic BC at surface for (a) anthropogenic  
815 contributions in January 2010, (b) anthropogenic contributions in July 2010, (c) open biomass  
816 burning contributions in January 2010, and (d) open biomass burning contributions in July  
817 2010.

818





819

820 Figure 7. Spatial distributions of contributions to Arctic BC at high altitudes for (a)  
821 anthropogenic contributions in January 2010, (b) anthropogenic contributions in July 2010, (c)  
822 open biomass burning contributions in January 2010, and (d) open biomass burning  
823 contributions in July 2010.

824